Mathematical Modeling of Heat Parameters of Photothermal Device

Boysori Yuldoshov, Mamasobir Tursunov, Gayrat Raimov, Shakhvoz Karshiev and Sirojiddin Toshpulatov
Termez State University, Barkamol Avlod Str. 43, 190111 Termez, Uzbekistan
b.yuldoshov10@mail.ru, mtursunov@tersu.uz, raimov.gayrat@mail.ru, shqarshiyev@tersu.uz, toshpulatovs@tersu.uz

Keywords: Solar Cell, Photovoltaic Panel, Photothermal Device, Heat Collector, Polycarbonate, Solar Radiation, Temperature.

Abstract: The article investigates hot water production by cooling a photovoltaic panel in a PV device. For this purpose, a parallel-channel polycarbonate heat collector was installed on the back surface of the PVT. The results obtained based on mathematical modelling of PVT thermal parameters are presented in the article. Mathematical modelling was performed based on Comsol multiphysics 6.1 integrated software. In mathematical modelling, the dependence of thermal energy obtained from PVT on radiation intensity, temperature and speed of cooling water was studied. Mathematical modeling results were compared with experimental results. According to the results of mathematical modelling, the maximum value of PV surface temperature was 47.6ºC in summer when the water speed was 0.001m/s. In the summer season, the results of the experiment conducted on the PVT device and mathematical modelling were compared. The results of experiments and mathematical modelling showed that the temperature of hot water difference by 2ºC. It was determined that 41.4 liters of hot water per hour is obtained from the PVT device.

1 INTRODUCTION

Solar energy is the largest and most environmentally friendly source of renewable energy. The amount of solar energy reaching the Earth is about 85PW. This is 500 times more than the world's power consumption (15TW) [1]. Solar energy can be converted into electrical and thermal energy using PV [2]. During the use of PV, its effectiveness decreases with the increase in temperature [3]. This process is related to the part of the radiation that is not absorbed by the solar elements and turns into heat. Various PVT models have been developed by researchers in recent years [4, 5, 6, 7]. Such devices differ in heat-absorbing (absorber) material, heat-carrying substance, and other physical parameters [8]. In [9], a complete description of the air and water configurations of the PVT system is presented. In [10], the electrical and thermal parameters of the PVT system, which consists of rectangular copper pipes on the back side of the polycrystalline PV, were described. In article [11], a flat water heater combined system with PVT is studied.

In [12], analytical expressions for energy balance equations and thermal parameters for various components of PVT were obtained. In some works, it is possible to see hydrodynamic equations in PVT [13, 14, 15, 16], and analyses obtained by mathematical modeling of electrical and thermal parameters [17, 18].

Since solar energy is a more sustainable source of energy than other renewable sources, it is important to follow research in this direction. In this article, the change in thermal parameters of the PVT system is analyzed using mathematical modelling.

2 METHODS AND MATERIALS

The temperature of the hot water obtained from the PVT mainly depends on the intensity of solar radiation and the surface of the area where the radiation falls. Therefore, reflectors installed in PVT also serve to increase thermal energy.

Figure 1 shows the solar radiation falling on the PV surface directly and through reflectors and the process of water heating in the PV heat collector.

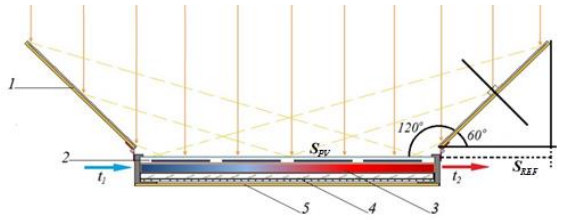

Figure 1: PVT reflectors are installed at an optimal angle. 1 – reflector, 2 – PV, 3 – heat collector, 4 – heat retaining materials, 5 – back cover.

The variation of PV and water temperatures at different velocities of water flowing through the channels of the heat collector of the PVT device was simulated using the integrated software Comsol multiphysics 6.1. In order to save computer RAM and reduce calculation time, mathematical modeling was performed for a part of the width of one solar cell in the direction of water flow channels (Fig. 2).

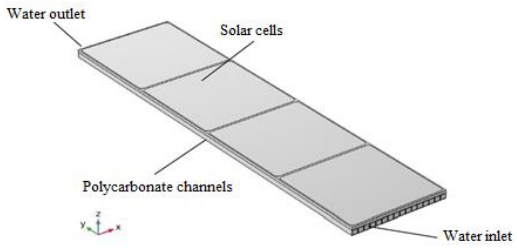

Figure 2: Part of PVT extracted for mathematical modelling.

In the modeling, hydrodynamic equations were solved to determine the dynamic quantities of flowing water in the channels. In the considered device, the speed of water flow varies in the range of 0.001-0.004 m/s. In this case, the following kinematic viscosity (1) is used for the Reynolds number (Re):

$$Re = \frac{V \cdot d}{v} \qquad (1)$$

herein, V – flow rating speed (m^3/s), d – channel size (m), v – kinematic viscosity (m^2/s). At a temperature of 40°C, the kinematic viscosity is equal to $0{,}659 \cdot 10^{-6} m^2/s$, will be less than 2300 at our chosen speed values.

At such small values of the Reynolds number, the water in the channels consists of a laminar flow. For this reason, we choose the "Laminar Flow" interface for the water flow in modeling.

The "Heat Transfer in Solids and Fluids" and "Surface-to-Surface Radiation" physics interfaces were used to simulate the heat exchange between fluid, PV, and the environment. In this case, the "Heat Transfer with Surface-to-Surface Radiation" multiphysics interface was used, which combines the description of "Heat transfer" and "Surface-to-surface radiation".

To describe the heat exchange of a water flow with a solid body, the "Laminar Flow (spf)" and "Heat Transfer in Solids and Fluids (ht)" interfaces through the "Nonisothermal Flow" nonisothermal flow multiphysics interface was connected.

For the convenience of modelling, we divide the input parameters into the following two types (Tables 1-2).

Table1: Geometric and dynamic parameters of the device.

Name of variables	Size (m)	Description
Wg	0.16	Width of PV
Lg	0.16	The length of the solar cell
H	0.00471	The thickness of PV
Ws	0.156	Width and height of the solar cell
Wk	0.0095	Water channel width
Hk	0.008	The height of the water channel
n	4	Solar element number
L	0.64 m	The length of PV
T_0	298.15 K	Initial water temperature
u_in	0.001 m/s	The speed of water entering the channels
Q_{water}	$1.28 \cdot 10^{-6}$ (m^3/s)	The amount of water coming out of the PVT in one second
N	16	Number of channels
M_{water}	4.608 kg	Mass of water heated in 1 hour

Table 2: Environment parameters.

Name of variables	Size	Description
T_{avg}	27 °C	Ambient temperature at start time
dT	3 °C	Ambient temperature gradient
Day	1	The day of the experiment
Month	7	The month of the experiment
Year	2021	The year of the experiment

Data from the ASHRAE Meteorological Database were used to account for changes in ambient temperature and solar activity. On July 1, 2021, the weather conditions in the city of Termez were taken from 10:00 a.m. to 4:00 p.m. The number of iterations for parametric research was 128, and the calculation time was 3 hours 31 minutes 23 seconds.

In the program, the following analytical expression was created to determine the temperature change in the movement of the earth about the sun during the day (2):

$$T_{amb} = T_{avg} + dT \cdot cos\left(\frac{x-14}{12} \cdot \pi\right), \quad (2)$$

here, Tamb is the ambient temperature (°C), Tavg – average temperature (°C), x – the time being viewed. The graph of this expression is presented in Figure 3.

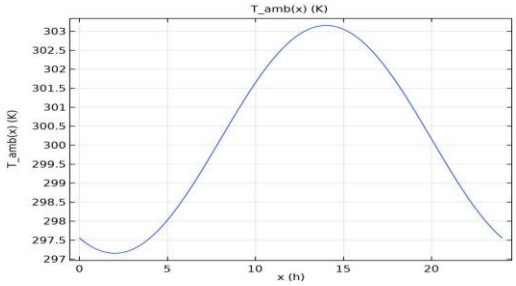

Figure 3: Changes in ambient temperature during the day.

Modeling was carried out in three-dimensional space. The model was implemented in an automated system for planar shear layers and turbulent flows. This model includes the least set of equations in the case where the unknown quantities are minimized for all-natural heat and flow processes [19, 20].

In the modelling, the blog of the nonstationary Navye-Stokes equation through nonlocal couplings was used in the Comsol multiphysics 6.1 platform and solved together with the continuity (3), (4):

$$\rho\frac{\partial u}{\partial t} + \rho(u\cdot\nabla)u = \nabla\cdot\left[-pI + K\right] + F \quad (3)$$

$$\rho\nabla\cdot u = 0 \quad (4)$$

therein, ρ – water density (kg/m^3), u – flow speed (m/s), I – impulse (kg•m/s), K – kinetic energy (J), F – external forces (N).

Boundary conditions were set as follows:

- the liquid does not slip on the walls of the channel, that is u=0, the flow speed is zero;
- the velocity at the entrance to the channels is directed along the normal of the entrance surface;
- the pressure difference at the exit from the channel is zero.

The developed equations for heat transfer in PV layers were used in the "Heat Transfer in Solids and Fluids" interface. The following heat balance equation and heat transfer (6) between layers were solved for solids:

$$\rho c_p\frac{\partial T}{\partial t} + \rho c_p u\nabla T + \nabla q = \sum Q_i \quad (5)$$

$$q = -k\nabla T \quad (6)$$

therein, u – flow speed of water (m/s), c_p – heat capacity (J/(kg•°C)), q – heat flux density (W/m^2), k – heat transfer coefficient (W/(m^2•°C)).

The following heat balance (7), (8) was solved for heat transfer between fluid and solid:

$$\rho c_p\frac{\partial u}{\partial t} + \rho c_p u\nabla T + \nabla q = Q + Q_p + Q_{vd} \quad (7)$$

$$\rho = \frac{p_A}{R_s T} \quad (8)$$

therein, Q – amount of heat (J), Q_p – spot heat quantity (J), Q_{vd} – Viscous dissipation (J), p_A – absolute pressure (Pa), R_s – Universal gas constant (J/kg•K). The effect of temperature on the density and viscosity of water was taken into account. It was considered that there is no heat exchange with the external environment (9):

$$-nu = 0 \quad (9)$$

n – normal to the wall. The following expression was used for the heat transfer to the external environment for the PV surface (10), (11):

$$-n\cdot q = q_0 \quad (10)$$

$$q_0 = k(T_{ext} - T) \quad (11)$$

therein, q – heat flux density (W/m^2), q_0 – internal heat flow (W/m^2), k – heat transfer coefficient W/(m^2•K), T_{ext} – exterior temperature (K).

The following quantities are available in the Comsol multiphysics 6.1 platform for the effects of incident radiation:

- solar radiation intensity;
- energy balance;
- Stefan-Bolsmann equation.

Functions indicating the ambient temperature were calculated as a result of the sum of radiation for all wavelengths, taking into account the geographical width of the selected area. The (12) - (16) were solved using the finite element method.

$$J_i = \varepsilon_i e_b(T) FEP_i(T) + \rho_{dj} G_i \quad (12)$$

$$G_j = G_{m,j} + G_{amb,j} + G_{ext,j} \quad (13)$$

$$G_{ambj} = F_{ambj}\varepsilon_{amb} e_b(T_{amb}) FEP_j(T_{amb}) \quad (14)$$

$$e_b(T) = n^2\sigma T^4 \quad (15)$$

$$FEP_j(T) = \frac{15}{\pi^4}\int_{c_2/(\lambda_{j-1}T)}^{c_2/(\lambda_j T)} \frac{x^3}{1-e^x}dx \quad (16)$$

therein, J_i – Intensity of radiation falling on the PV surface (W/m^2), ε_i – surface irradiation capacity, e_b – grayness of the surface, FEP_i – seasonal radiation conditions of the area, ρ_{dj} – coefficient of reflection, G_i – surface radiation intensity (W/m^2), G_{mj} – mutual surface radiation (W/m^2), $G_{amb,j}$ – environmental radiation (W/m^2), G_{ext} – external radiation (W/m^2), $F_{amb,j}$ – environmental factor, ε_i – environmental emissivity, n – light refraction indicator, c_2 – heat capacity (J/(kg•°C)), λ_j – thermal conductivity (W/m^2).

3 RESULTS AND DISCUSSION

The number of solar elements and the channel length were considered in mathematical modelling. Determined experimentally 0.001m/s value was given for the velocity of water entering the cooling system channels. Primarily, the surface heating of a 640mm long solar panel piece consisting of 4 elements was studied at four different time points (Fig. 4).

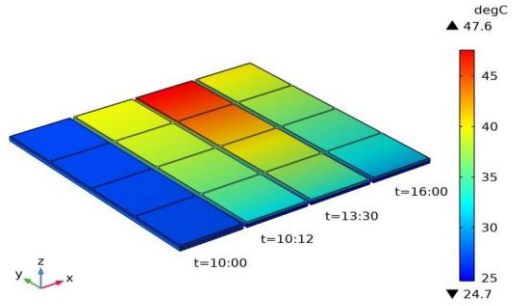

Figure 4: Change of PV surface temperature when water speed u_in(1)=0.001 m/s.

During periods of perpendicular solar radiation, the water outlet temperature of PVT reaches its maximum value of 47ºC. In the rest of the time, the outgoing water temperature is 41-42ºC. The velocity of the water inside the channels is small and the thickness of the polycarbonate wall is 0.5mm, so the temperature of the water is close to the temperature of the PV. It differs by 1-1.5ºC at most.

Figure 5 shows the change in water temperature in the channels of the PVT heat collector during the day. It can be seen from the picture that the difference between the temperature of the PV surface and the temperature of the water shown in Figure 5 was equal to 1.1^{0}C. This situation is very close to the experimental result, with a difference of 1.5-2ºC due to the presence of external temperature and wind speed.

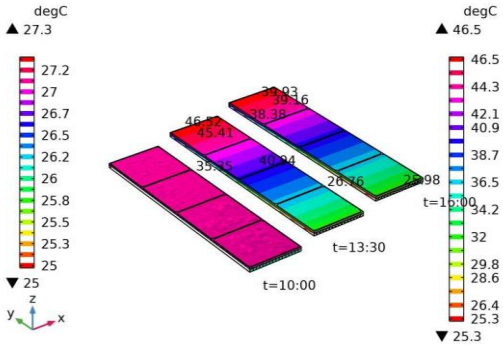

Figure 5: Change of water temperature at a water speed u_in(1)=0.001 m/s.

Figure 6 shows the change in water temperature at different water speeds under the same conditions. It can be seen from the figure that when the water speed is 0.001 m/s, the PVT surface temperature is 47ºC, while the exit water temperature is 45ºC.

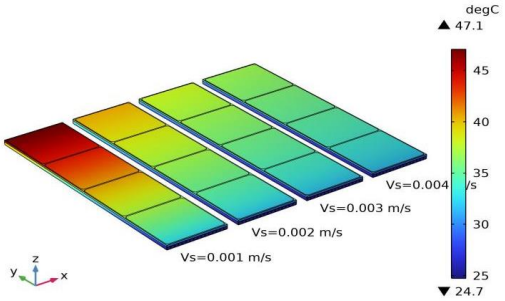

Figure 6: Change in water temperature at different water speeds under the same conditions.

As a result of changes in water density, viscosity and pressure due to the temperature gradient along the length of the channels, an increase in water flow speed is observed. The speed of water in the channels increases along the length of the PV and reaches 0.00199 m/s almost twice due to the loss of the pressure difference at the outlet (Fig. 7-8).

Figure 9 shows the absorption of radiation in the heat collector through the PV surface. It shows the amount of radiation converted into heat during the day in one line of PV when the water flow speed is 0.003 m/s.

Figure 10 shows the absorption of solar radiation at different water flow rates in a PVT heat collector under the same conditions. In the graph, the result of the above opinion was approved.

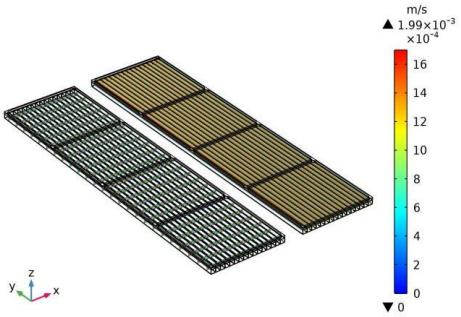

Figure 7: Increase in water speed in channels, t=13:30.

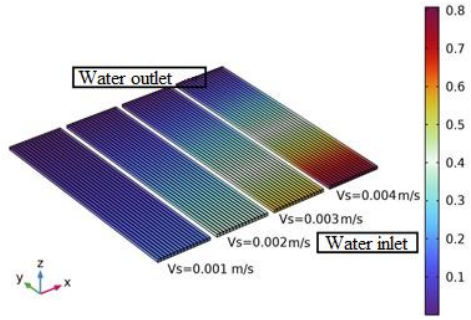

Figure 8: Change of pressure in channels at different speeds, t=13:30.

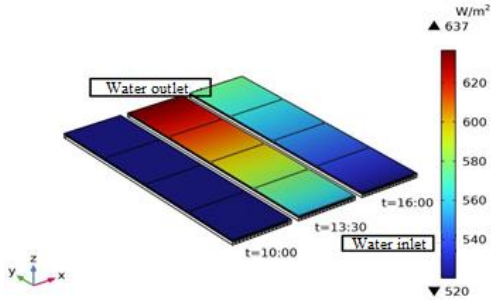

Figure 9: Absorption of solar radiation in PVT, (W/m^2).

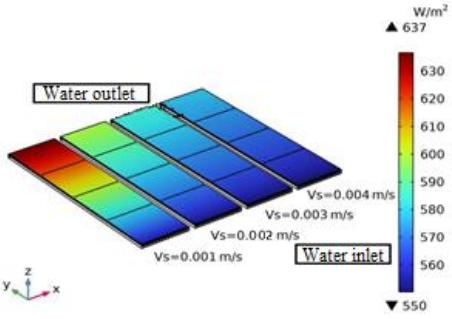

Figure 10: Absorption of solar radiation in FIB at different water speeds, (W/m^2).

The thickness of the normal to the surface of the device consisting of PV and cooling system is 14.71 mm. The walls of the polycarbonate channel are 0.5 mm thick. The width and the height of the channel are 5 mm and 8mm respectively. Figure 11 shows the temperature change in polycarbonate, water, polycarbonate and solar elements as a result of the heat exchange process in the layers due to the absorption of the radiation falling on the PV surface. At a water speed of 0.001 m/s, the temperatures ranged from 31°C to 34.4°C in QE1, 32°C to 35°C in QE2, 33.3°C to 37.4°C in QE3, and 37.2°C to 41.2°C in QE4 can be seen to change.

Figure 12 shows the variation of the PV surface temperature along the length of the channel during the day. Under the same conditions, the temperature of the solar cell will be from 40^{o}C to 47.5^{o}C at values of water flow velocity of 0.001-0.002 m/s. The arrangement of four solar cells along the length of the channel can be called the optimal option.

Figure 13 can be used to determine the optimal value of the water flow rate for the use of the cooling system as a heat collector. It can be seen from the picture that for use as a heat collector, the flow rate in the channels of 0.001m/s gives the possibility of receiving water at a temperature of 39^{o}C-40^{o}C.

4 CONCLUSIONS

The mathematical modeling of thermal parameters in photovoltaic-thermal (PV/T) devices plays a key role in understanding and improving the processes within combined systems. For this purpose, modeling of thermal processes in a PVT device which has a polycarbonate heat collector was carried out. When the speed of water in the PVT channel is 0.001m/s, the temperature of the PV surface is 47.6°C, and the temperature of the outgoing water is 46.5°C. When the reflector is installed at the optimal angle, the temperature of the PV surface is 61.2°C, and the temperature of the outgoing water is 58°C. Also, the temperature change in the first solar cell (QE1) when cold water passes through the heat collector is 31^{o}C - 34.4^{o}C, in QE2 it is 32^{o}C - 35^{o}C, in QE3 it is 33.3^{o}C - 37.4^{o}C and in QE4 it is 37.2^{o}C - 41.2^{o}C, determined. These results differed by 2^{0}C from the experimental result. It was found that 41.4 litres of hot water per hour was taken from the device. By increasing the incoming water consumption, electricity losses are reduced, however, the decreasing outgoing water temperature has been proven based on experimental and modeling results.

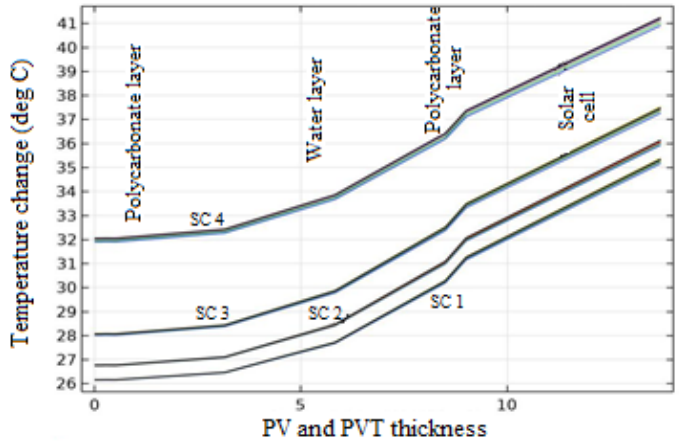

Figure 11: Variation of PV temperature during the day.

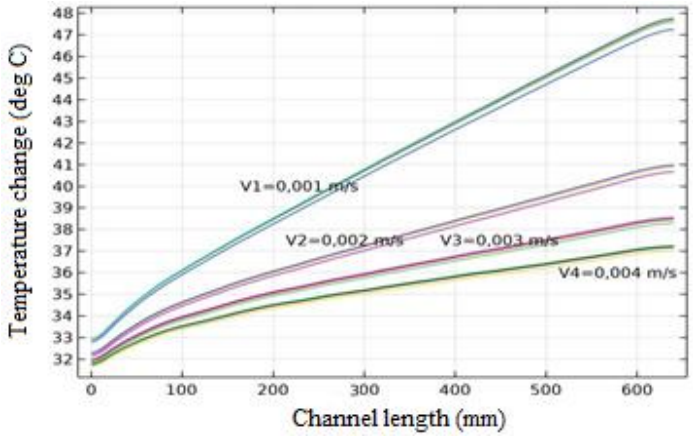

Figure 12: Variation of temperature on the surface of PV during the day.

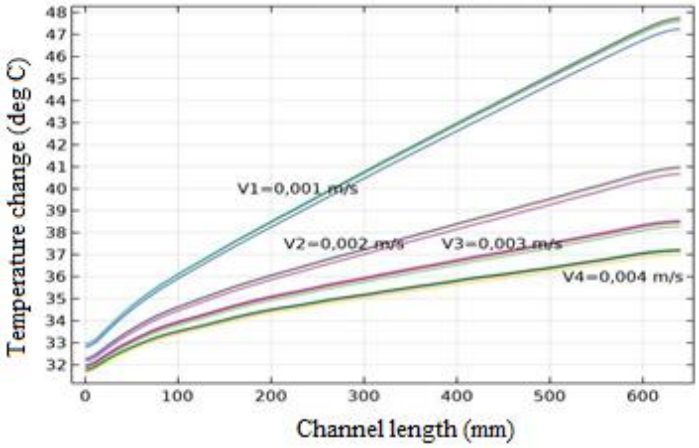

Figure 13: Change in water temperature in the channel.

REFERENCES

[1] M. Khamooshi, H. Salati, F. Egelioglu, A. Hooshyar Faghiri, J. Tarabishi, and S. Babadi, "A review of solar photovoltaic concentrators," Int. J. Photoenergy, vol. 2014, pp. 1-17.

[2] M. Tursunov, K. Sabirov, T. Axtamov, U. Abdiyev, B. Yuldoshov, J. Khaliyarov, S. Bobomuratov, and S. Toshpulatov, "Analysis of electric and thermal efficiency of crystal silicon small power suppliers," in Proc. Int. Conf. Appl. Innov. IT, vol. 11, no. 2, 2023, pp. 167-171.

[3] R. Muminov, M. Tursunov, Kh. Sabirov, Sh. Abilfayziyev, B. Yuldoshov, and S. Toshpulatov, "Testing of crystalline silicon-based photoelectric and photothermal batteries in real climate conditions and comparison of parameter changes," J. Phys.: Conf. Ser., vol. 2388, 2022, 012128. doi: 10.1088/1742-6596/2388/1/012128.

[4] W. He, J. Zhou, C. Chen, and J. Ji, "Experimental study and performance analysis of a thermoelectric cooling and heating system driven by a photovoltaic/thermal system in summer and winter operation modes," Energy Convers. Manag., vol. 84, 2014, pp. 41-49.

[5] A. Monjezi, Y. Chen, R. Vepa, A. Kashyout, G. Hassan, H. Fath, and M. Shaheed, "Development of an off-grid solar energy powered reverse osmosis desalination system for continuous production of freshwater with integrated photovoltaic thermal (PVT) cooling," Desalination, vol. 495, 2020, pp. 1-7.

[6] H. Nasef, S. Nada, and H. Hassan, "Integrative passive and active cooling system using PCM and nanofluid for thermal regulation of concentrated photovoltaic solar cells," Energy Convers. Manag., vol. 199, 2019, pp. 1-15.

[7] U. Sajjad, M. Amer, H. Ali, A. Dahiya, and N. Abbas, "Cost-effective cooling of photovoltaic modules to improve efficiency," Case Stud. Therm. Eng., vol. 14, 2019, pp. 1-7.

[8] S. Bhakre, P. Sawarkar, and V. Kalamkar, "Performance evaluation of PV panel surfaces exposed to hydraulic cooling – A review," Sol. Energy, vol. 224, 2021, pp. 1193-1209.

[9] R. Avezov, J. Akhatov, and N. Avezova, "A review on photovoltaic-thermal (PV-T) air and water collectors," Appl. Sol. Energy, vol. 47, no. 3, 2011, pp. 169-183.

[10] A. Alzaabi, K. Badawiyeh, O. Hantoush, and A. Hamid, "Electrical/thermal performance of hybrid PV/T system in Sharjah, UAE," Int. J. Smart Grid Clean Energy, vol. 3, no. 4, 2014, pp. 385-389.

[11] M. Arefin, "Analysis of an integrated photovoltaic thermal system by top surface natural circulation of water," Front. Energy Res., vol. 7, 2019, pp. 1-10.

[12] F. Sobhnamayan, F. Sarhaddi, M. Alavi, S. Farahat, and J. Yazdanpanahi, "Optimization of a solar photovoltaic thermal (PV/T) water collector based on exergy concept," Renew. Energy, vol. 68, 2014, pp. 356-365.

[13] F. Yazdanifard, E. Ebrahimnia-Bajestan, and M. Ameri, "Investigating the performance of a water-based photovoltaic/thermal (PV/T) collector in laminar and turbulent flow regime," Renew. Energy, vol. 99, 2016, pp. 295-306.

[14] Z. Ul Abdin and A. Rachid, "Bond graph modeling of a water-based photovoltaic thermal (PV/T) collector," Sol. Energy, vol. 220, 2021, pp. 571-577.

[15] S. Prasetyo, A. Prabowo, and Z. Arifin, "The use of a hybrid photovoltaic/thermal (PV/T) collector system as a sustainable energy-harvest instrument in urban technology," Heliyon, vol. 9, 2023, pp. 1-25.

[16] D. Luca, A. Caldarelli, E. Gaudino, E. Gennaro, M. Musto, and R. Russo, "Modeling of energy and exergy efficiencies in high vacuum flat plate photovoltaic–thermal (PV–T) collectors," Energy Rep., vol. 9, 2023, pp. 1044-1055.

[17] E. Touti, M. Masmali, M. Fterich, and H. Chouikhi, "Experimental and numerical study of the PVT design impact on the electrical and thermal performances," Case Stud. Therm. Eng., vol. 43, 2023, pp. 1027-1032.

[18] M. Attia, A. Khelifa, O. Abdulmajeed, and M. Arıcı, "Thermal analysis on the performance of a finned hybrid bi-fluid PVT system," Therm. Sci. Eng. Prog., vol. 45, 2023, pp. 1021-1035.

[19] P. Bradshaw, "Turbulent secondary flows," Annu. Rev. Fluid Mech., vol. 19, 1987, pp. 53-74.

[20] I. Jurayev, I. Yuldoshev, and Z. Jurayeva, "Results of study of photovoltaic thermal battery based on thin-film module by modeling and computational methods," in Proc. Int. Conf. Appl. Innov. IT, vol. 12, no. 1, 2024, pp. 243-249. doi: 10.25673/115707.

APPENDIX

The list of abbreviations used in this paper is given below:

PV	photovoltaic panel
PVT	photothermal panel